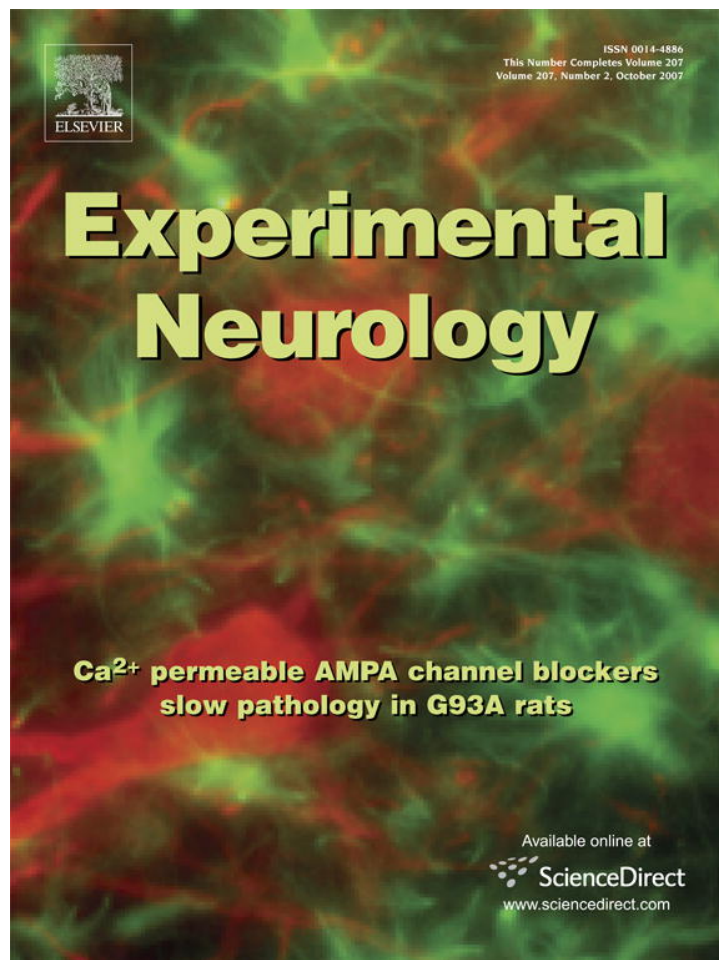


Provided for non-commercial research and education use.
Not for reproduction, distribution or commercial use.



This article was published in an Elsevier journal. The attached copy is furnished to the author for non-commercial research and education use, including for instruction at the author's institution, sharing with colleagues and providing to institution administration.

Other uses, including reproduction and distribution, or selling or licensing copies, or posting to personal, institutional or third party websites are prohibited.

In most cases authors are permitted to post their version of the article (e.g. in Word or Tex form) to their personal website or institutional repository. Authors requiring further information regarding Elsevier's archiving and manuscript policies are encouraged to visit:

<http://www.elsevier.com/copyright>



ELSEVIER

Available online at www.sciencedirect.com

Experimental Neurology 207 (2007) 227–237

**Experimental
Neurology**

www.elsevier.com/locate/yexnr

Minocycline protects the blood–brain barrier and reduces edema following intracerebral hemorrhage in the rat

Jason K. Wasserman, Lyanne C. Schlichter*

Toronto Western Research Institute, University Health Network, Toronto Ontario, Canada M5T 2S8
 Department of Physiology, University of Toronto, Toronto Ontario, Canada M5T 2S8

Received 30 March 2007; revised 19 June 2007; accepted 22 June 2007
 Available online 18 July 2007

Abstract

Intracerebral hemorrhage (ICH) results from rupture of a blood vessel in the brain. After ICH, the blood–brain barrier (BBB) surrounding the hematoma is disrupted, leading to cerebral edema. In both animals and humans, edema coincides with inflammation, which is characterized by production of pro-inflammatory cytokines, activation of resident brain microglia and migration of peripheral immune cells into the brain. Accordingly, inflammation is an attractive target for reducing edema following ICH. In the present study, BBB damage was assessed by quantifying intact microvessels surrounding the hematoma, monitoring extravasation of IgG and measuring brain water content 3 days after ICH induced by collagenase injection into the rat striatum. In the injured brain, the water content increased in both ipsilateral and contralateral hemispheres compared with the normal brain. Quantitative real-time RT-PCR revealed an up-regulation of inflammatory genes associated with BBB damage; IL1 β , TNF α and most notably, MMP-12. Immunostaining showed MMP-12 in damaged microvessels and their subsequent loss from tissue surrounding the hematoma. MMP-12 was also observed for the first time in neurons. Dual-antibody labeling demonstrated that neutrophils were the predominant source of TNF α protein. Intraperitoneal injection of the tetracycline derivative, minocycline, beginning 6 h after ICH ameliorated the damage by reducing microvessel loss, extravasation of plasma proteins and edema; decreasing TNF α and MMP-12 expression; and reducing the numbers of TNF α -positive cells and neutrophils in the brain. Thus, minocycline, administered at a clinically relevant time, appears to target the inflammatory processes involved in edema development after ICH.

© 2007 Elsevier Inc. All rights reserved.

Keywords: Stroke; Microvessels; Real-time RT-PCR; Inflammatory cytokines; CNS inflammation; Blood–brain barrier disruption; Brain edema

Introduction

Intracerebral hemorrhage (ICH) accounts for 10–30% of all strokes, with as much as 30–40% mortality by one month (Rincon and Mayer, 2004). After ICH, cerebral edema begins within hours, can last for weeks and is thought to contribute to neurological deterioration by increasing intracranial pressure or causing a shift in midline structures (Mayer and Rincon, 2005). Vasogenic edema is prevalent after ICH (Rincon and Mayer, 2004) and results from pathological changes in the blood–brain barrier (BBB) and consequent fluid movement from the vasculature to the extracellular space of the brain. Less important is

the cytotoxic edema resulting from increased water uptake by brain cells (especially neurons). The BBB serves as the anatomical barrier between the blood and brain parenchyma and is comprised of endothelial cells, astrocytic end-feet, pericytes and a specialized basement membrane (the basal lamina) that serves as a scaffold supporting the physical integrity of the microvasculature. Although the basal lamina is clearly involved in BBB breakdown after ischemic stroke (Hamann et al., 2002), its role after ICH remains unresolved.

The inflammatory response following ICH, like other forms of brain injury, is characterized by production of several molecules that can disrupt the BBB (Wang and Dore, 2006). Moreover, because the delayed onset of both inflammation and vasogenic edema allows more time for patients to reach hospital after the onset of ICH, they are attractive therapeutic targets. In other forms of brain injury, the initial inflammatory response is

* Corresponding author. MC 9-417, 399 Bathurst Street, Toronto Ontario, Canada M5T 2S8. Fax: +1 416 603 5745.

E-mail address: schlicht@uhnres.utoronto.ca (L.C. Schlichter).

orchestrated by the cytokines, TNF α and IL1 β , which are up-regulated within hours (Barone and Feuerstein, 1999; Hua et al., 2006; Mayne et al., 2001b,a; Qureshi et al., 2001), but less is known about their temporal and spatial expression after ICH. While the 'resting' BBB severely limits movement of fluid, macromolecules and cells into the brain, TNF α and IL1 β 'activate' the endothelium, increase its permeability and allow adhesion and entry of peripheral immune cells (Feuerstein et al., 1998; Middleton et al., 2002; Zhang et al., 2000). Transmigrating neutrophils in particular, produce cytotoxic molecules including inflammatory cytokines, reactive oxygen species and matrix metalloproteinases (MMPs) (Scholz et al., 2007). MMP production, also ascribed to endothelial cells, microglia/macrophages, astrocytes and neurons, can further damage the BBB by degrading the basal lamina of cerebral blood vessels (Rosenberg, 2002). Following ICH in the rat, several MMPs are up-regulated (Power et al., 2003; Wells et al., 2005), but their impact on cerebral blood vessels and BBB breakdown has yet to be assessed.

Minocycline, a semi-synthetic tetracycline derivative, is of particular therapeutic interest for CNS disorders because it has a high oral bioavailability, superior BBB penetration and is well tolerated by humans, where it has been used for decades to treat bacterial infections (Stirling et al., 2005; Yong et al., 2004). Its efficacy has been demonstrated in animal models of acute brain injury, including focal ischemia (Yrjanheikki et al., 1998, 1999), ICH (Power et al., 2003), traumatic brain injury (Sanchez Mejia et al., 2001) and spinal cord injury (Wells et al., 2003), and proposed mechanisms include very diverse effects on several cell types. With respect to inflammation, it can inhibit activation and migration of inflammatory cells, and after ICH in the rat it inhibits macrophages/microglia (Power et al., 2003; Wasserman and Schlichter, 2007) and neutrophils (Wasserman and Schlichter, 2007). Minocycline has been reported to reduce specific cytokines (TNF α , IL1 β) and MMPs (Elewa et al., 2006; Power et al., 2003) that have been implicated in BBB damage, and in animal models of ischemic stroke it can reduce BBB damage (Maier et al., 2006; Yenari et al., 2006).

The present work builds on two studies of collagenase-induced ICH in the rat striatum. Power and colleagues (2003) described the time course of MMP mRNA expression distal to the hematoma (2–4 mm) and effects of early treatment with minocycline (starting at 1 h) on MMP up-regulation and the neurological outcome. In the same model (Wasserman and Schlichter, 2007), we recently investigated the spatial and temporal relationship between neuron death and inflammation, and effects of minocycline treatment begun at a later, more clinically relevant time (6 h); i.e., after the hematoma had reached its maximal size. Using the same model, we now assess the effects of delayed minocycline treatment on blood vessel deterioration and edema, and on time-dependent changes in several key molecules involved in these events. BBB damage was monitored by counting the number of intact microvessels surrounding the hematoma (Hamann et al., 2002), assessing the extravasation of IgG into the brain (Tanno et al., 1992), and measuring brain water content 3 days after ICH onset. Then, because a prominent inflammatory response occurs in the tissue immediately adjacent to the hematoma, we monitored gene

expression in and around the damage site with and without minocycline treatment and began at an earlier time than previously examined. Expression of IL1 β , TNF α , MMP-3, MMP-9, MMP-12 and the microglia/macrophage marker, complement receptor 3 were monitored at 6 h, 1 day and 3 days after ICH, using quantitative real-time RT-PCR. Finally, for the two genes whose up-regulation was reduced by minocycline (TNF α , MMP-12), we used immunohistochemistry to determine which cell types expressed the proteins. We show that TNF α increased early, mainly in neutrophils; whereas, MMP-12 increased later in damaged microvessels surrounding the hematoma. Delayed minocycline treatment reduced: microvessel loss, plasma protein extravasation and edema; expression of TNF α and MMP-12; and the number of TNF α -positive cells and neutrophils in the brain. These findings support a model whereby immune cells produce TNF α , which leads to an increase in MMP-12 in microvessels surrounding the hematoma, causing further degradation of the basal lamina and BBB disruption.

Methods

Intracerebral hemorrhage and minocycline treatment

Intracerebral hemorrhage was induced in the striatum of male Sprague–Dawley rats (300–350 g, $n=40$) as previously described (Rosenberg et al., 1990; Wasserman and Schlichter, 2007). All procedures were approved by the University Health Network animal care committee, in accordance with guidelines established by the Canadian Council on Animal Care. Rats were anesthetized using isoflurane (3% induction, 1.5% maintenance) and placed in a stereotaxic frame. Under aseptic conditions, a 1-mm diameter burr hole was drilled in the skull (0.2 mm anterior and 3 mm lateral to bregma) and a 30-gauge needle was lowered into the right caudate putamen (6 mm ventral from the skull surface). A micropump (Micro4, World Precision Instruments, Sarasota, FL) delivered 0.25 U of bacterial type IV collagenase (Sigma, Oakville, ON) in 0.5 μ L saline, at 250 nL/min, after which the needle was left in place for 5 min to prevent solution reflux. For sham-operated controls ($n=24$), the same procedures were performed, except that collagenase was omitted from the saline. Core temperature was maintained at 37 °C using an electric heating pad throughout surgery and recovery; animals regained consciousness within 10 min. This procedure resulted in reproducible lesions that were restricted to the striatum (see Fig. 1A) except in a few animals, where a small amount of blood was also observed in the surrounding white matter. No animals died as a result of any of the surgeries.

Minocycline (Sigma) was stored at 4 °C until freshly prepared in sterile saline for intraperitoneal injection (45 mg/kg) at 6 h and 1 and 2 days after ICH onset. Control animals received an equivalent amount of sterile saline. Similar minocycline doses have been used in models of hemorrhagic (Power et al., 2003; Szymanska et al., 2006; Wasserman and Schlichter, 2007) and ischemic stroke (Hewlett and Corbett, 2006; Yrjanheikki et al., 1998). Previous studies began treatment sooner (i.e., at 1 h; Power et al., 2003; at 3 h; (Szymanska et al., 2006), while our studies

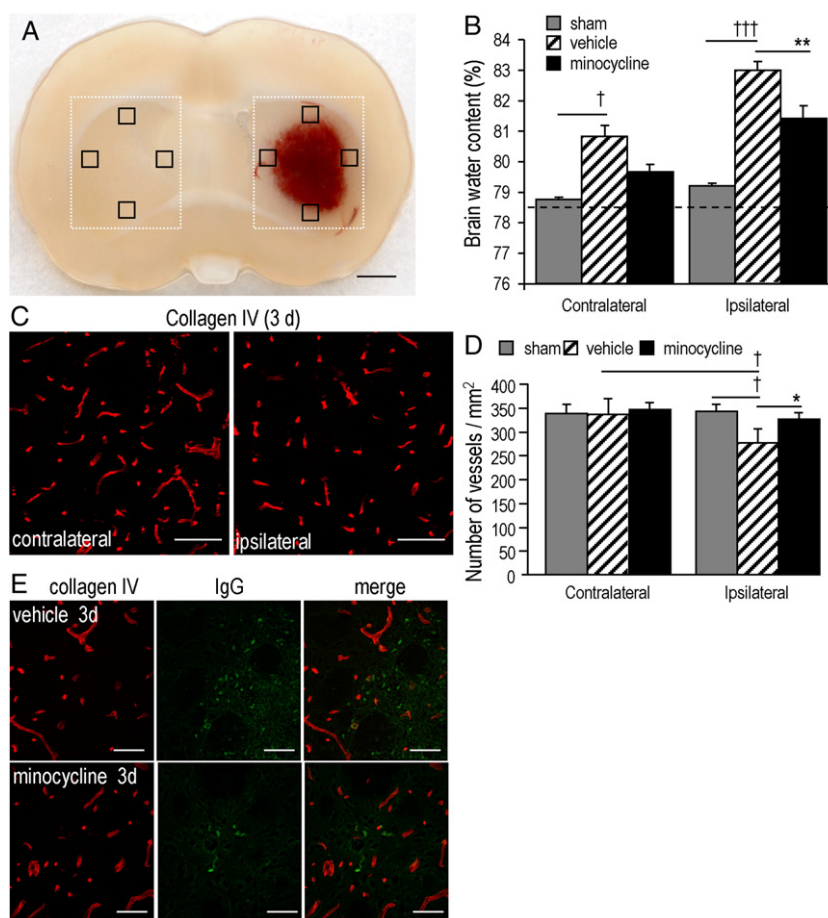


Fig. 1. Minocycline reduces cerebral edema and loss of microvessels after intracerebral hemorrhage (ICH). (A) A typical hematoma in a section sliced coronally through the middle of the hematoma 1 day after injection into the striatum of 0.25 U bacterial type IV collagenase. For each condition, microvessels and cells were counted in four randomly selected grids (black boxes show examples) at the edge of the hematoma and in a homologous region of the contralateral striatum. All bar graphs show the average of four grids for the number of animals indicated below. The white dotted boxes show the approximate regions harvested for real-time RT-PCR. Scale bar, 1 mm. (B) At 3 days after ICH onset, edema (i.e., percent brain water) was increased in the ipsilateral hemisphere ($^{\dagger\dagger\dagger}p < 0.001$) and to a lesser degree in the contralateral hemisphere ($^{\dagger}p < 0.05$; $n = 7$) compared with sham-operated controls ($n = 3$). The dashed line indicates the mean water content of the striatum of naïve rats ($n = 6$), not subjected to any surgical procedure. Minocycline treatment (i.p. injections at 6 h, 1 day and 2 days, see Methods) reduced edema in the ipsilateral hemisphere ($^{**}p < 0.01$; $n = 8$) compared with vehicle-treated animals ($n = 8$). (C) Representative confocal images at 3 days after ICH onset, showing microvessels, stained with an antibody against collagen type IV, in the contralateral striatum and at the edge of the hematoma. Scale bars, 100 μm . (D) At 3 days, microvessels were counted and averaged from 4 grids for each of 4 rats per treatment group. Vehicle-treated rats had fewer microvessels at the edge of the hematoma, compared with the contralateral striatum of the same animal ($^{\dagger}p < 0.05$) or the ipsilateral striatum of sham-operated animals ($^{\dagger}p < 0.05$). Minocycline reduced microvessel loss at the edge of the hematoma compared with vehicle-treated controls ($^{*}p < 0.05$). (E) Representative confocal images at 3 days after ICH onset. Microvessels are stained with an antibody against collagen type IV and anti-IgG antibody shows extravasation of plasma immunoglobulin G at the edge of the hematoma. Scale bars, 100 μm .

have delayed the initial treatment to a more clinically relevant time (Power et al., 2003; Szymanska et al., 2006; Wasserman and Schlichter, 2007; present study).

Brain water content

Edema was assessed by measuring brain water content, with some modifications to an earlier protocol (MacLellan et al., 2004). Three days after ICH onset, animals ($n = 7$ –8 per treatment group) were overdosed with isoflurane, decapitated and their brains were removed. The cerebellum and brain stem were removed, the remaining hemispheres were divided along the midline and their wet weights determined. Dry weights were obtained after drying for 24 h in an oven at 100 °C. Water content was expressed as a percentage of the wet weight: (wet weight –

dry weight)/(wet weight) $\times 100$. Brain water content was also measured in sham-operated animals receiving a saline injection and in naïve animals that received no surgery.

Immunohistochemistry

Animals were sacrificed by an overdose of isoflurane at 3 days ($n = 8$) after the onset of ICH, and then perfused through the heart with 100 mL phosphate-buffered saline (PBS) followed by 60 mL of fixative (4% paraformaldehyde, 2% sucrose in PBS; pH 7.5). Dissected brains were stored in the same fixative at 4 °C overnight, followed by 10% sucrose for 24 h, and 30% sucrose for 48 h. Fixed brains were cut coronally through the needle entry site (easily identified on the brain surface), and at 4 mm anterior and 4 mm posterior to that plane. Frozen brain sections

(16 μm thick) were made using a cryostat (JungCM 3000, Leica, Richmond Hill, ON) and were stored at $-80\text{ }^{\circ}\text{C}$ until used.

Microvessels and cells were visualized by immunohistochemistry on adjacent frozen sections using a confocal fluorescence microscope (Zeiss LSM 510 META, Oberkochen, Germany). Counts were made by a blinded observer and averaged over four grids ($368\times 368\text{ }\mu\text{m}$ each) adjacent to the hematoma and in homologous regions of the contralateral striatum (see boxed areas in Fig. 1A), with 4–8 animals per treatment group, as indicated. Microvessels were identified with an antibody against collagen type IV (rabbit polyclonal, 1:250, Abcam, Cambridge, MA), which is a major constituent of the basal lamina of cerebral vessels (Hamann et al., 2002). Extravasation of IgG was detected in frozen brain sections with an antibody against rat IgG (donkey polyclonal, 1:100, Jackson Laboratories, West Grove, PA). Antibodies used to identify cell types were anti-microtubule-associated protein-2 (MAP2; rabbit polyclonal; 1:1000; Chemicon, Temecula, CA) for neurons, 'ionized calcium-binding adapter-1' (Iba1; rabbit polyclonal; 1:1000; Wako, Japan) for microglia/macrophages and myeloperoxidase (MPO; rabbit polyclonal; 1:300, Dako-Canada, Mississauga, ON) for neutrophils. Cell counts were automated using a cell counting tool in ImageJ software (NIH, version 1.33k). In order to identify the cellular source and location of MMP-12 and $\text{TNF}\alpha$, double labeling was performed with one of these cell markers and an antibody against MMP-12 (mouse monoclonal; 1:150; Minneapolis, MN) or $\text{TNF}\alpha$ (Armenian hamster polyclonal; 1:100; eBioscience, San Diego, CA). For secondary antibody labeling, the sections were washed in PBS ($3\times$, 10 min each) and incubated (2 h, room temperature) in PBS containing 3% normal goat serum, 0.3% Triton X-100 and either a Cy3-conjugated anti-mouse antibody (1:500; Jackson Laboratories) and/or an Alexa 488-conjugated anti-rabbit antibody (1:500; Molecular Probes, Burlington, ON), as appropriate.

Quantitative real-time reverse transcriptase polymerase chain reaction (qRT-PCR)

To assess temporal changes in gene expression, mRNA levels were monitored by real-time RT-PCR (Bustin and Nolan, 2004; Kaushal et al., 2007). Brain tissue was rapidly harvested after rats were sacrificed by an overdose of isoflurane, and then perfused through the heart with 100 mL PBS. Dissected brains were cut coronally, 2 mm anterior and 2 mm posterior to the needle entry site (easily identifiable on the surface of the brain) and were divided into separate hemispheres along the midline. Next, the striatum on each side of the brain was separated from the surrounding white matter and cortex, and used for RNA extraction. In ICH animals, this area included most of the hematoma and a surrounding region of striatal tissue. Primers were designed with the 'Primer3Output' program (http://frodo.wi.mit.edu/cgi-bin/primer3/primer3_www.cgi) (Table 1). RNeasy mini kits (Qiagen, Mississauga, ON) were used to isolate RNA after degrading any contaminating DNA with DNaseI (0.1 U/ml, 15 min, $37\text{ }^{\circ}\text{C}$; Amersham Biosciences, Baie d'Urfe, PQ). A two-step reaction was performed according to the manufacturer's instructions (Invitrogen); i.e., total RNA (1 μg

Table 1
Primers used for real-time RT-PCR

Gene	GenBank accession #	Primer sequences
CR3	NM012711	TGCTGAGACTGGAGGCAAC (FP) CTCCCCAGCATCCTTGTTT (RP)
IL1 β	NM031512	TGACCCATGTGAGCTGAAAG (FP) AGGGATTTTGTCTGTTGCTTG (RP)
MMP-3	NM133523	TCCACAGAATCCCCTGA (FP) CGCCAAAAGTGCCTGTCT (RP)
MMP-9	NM031055	CTGCCTGCACCACTAAAGG (FP) GAAGACGAAGGGGAAGACG (RP)
MMP-12	NM053963	CTGGGCAACTGGACACCT (FP) CTACATCCGCACGCTTCA (RP)
$\text{TNF}\alpha$	NM012675	GCCACGTCGTAGCAAAC (FP) GCAGCCTTGTCCCTTGAA (RP)
HPRT1	XM343829	CAGTACAGCCCCAAAATGGT (FP) CAAGGGCATATCCAACAACA (RP)

FP: forward primer; RP: reverse primer.

was reverse transcribed in 20 μL volume using 200 U of SuperScriptII RNase H-reverse transcriptase, with 0.5 mM dNTPs (Invitrogen) and 0.5 μM oligo dT (Sigma). Amplification was performed on an ABI PRISM 7700 Sequence Detection System (PE Biosystems, Foster City, CA) at $95\text{ }^{\circ}\text{C}$ for 10 min, followed by 40 cycles at $95\text{ }^{\circ}\text{C}$ for 15 s, $56\text{ }^{\circ}\text{C}$ for 15 s and $72\text{ }^{\circ}\text{C}$ for 30 s. 'No-template' and 'no-amplification' controls were included for each gene, and melt curves showed a single peak, confirming specific amplification (Bustin and Nolan, 2004). The threshold cycle (C_T) for each gene was determined, normalized against the housekeeping gene, hypoxanthine guanine phosphoribosyl transferase (HPRT1) and expressed as fold changes relative to sham-operated, time-matched controls (without ICH). At each time point (6 h, 1 day and 3 days), rats with ICH were compared with time matched sham-operated controls, and with rats receiving an ICH plus minocycline.

Statistical analyses

Where appropriate, data are expressed as the mean \pm SD for the number of animals indicated. ANOVA, with Bonferroni post hoc correction was used to compare differences between treatment groups, with $p < 0.05$ considered significant.

Results

Minocycline reduces cerebral edema and the loss of microvessels

Cerebral edema peaks at 3–4 days after ICH onset in the rat (see Discussion); thus, we measured the brain water content at 3 days (Fig. 1B). Naïve rats, not subjected to any surgical procedure, had a brain water content of $78.65\pm 0.11\%$ ($n=6$), whereas sham-operated rats (saline-injected, no collagenase; $n=3$) had a brain water content of $79.2\pm 0.09\%$ in the ipsilateral hemisphere and 78.9 ± 0.06 in the contralateral hemisphere. The cerebral hemisphere was used as the internal control, rather than the cerebellum, which had lower water content ($\sim 76\%$). After ICH, the water content of vehicle-treated rats ($n=7$) significantly increased compared with sham-operated rats: to $83.00\pm 0.29\%$

in the ipsilateral hemisphere ($p < 0.001$), and $80.84 \pm 0.31\%$ in the contralateral hemisphere ($p < 0.05$). Minocycline, administered 6 h after ICH onset, reduced the water content in the ipsilateral hemisphere to $81.44 \pm 0.39\%$ compared with vehicle-treated controls ($p < 0.01$; $n = 8$). The water content in the contralateral hemisphere was also decreased (to $79.65 \pm 0.26\%$) but did not reach statistical significance.

Vasogenic edema results from degradation of the basal lamina, which disrupts the physical integrity of the BBB and allows serum proteins and fluid to enter the brain. First, basal lamina degradation was monitored by counting the number of intact vessels in the surrounding parenchyma (Hamann et al., 2002). This method – in contrast to the frequently used extravasation of Evans Blue dye – allowed the spatial and anatomical association of specific proteins with damaged vessels. Immunostaining for collagen type IV showed microvessel disruption in the ipsilateral striatum of vehicle-treated ICH animals 3 days after ICH onset (Fig. 1C). There were significantly fewer intact microvessels in the ipsilateral striatum surrounding the hematoma ($276 \pm 13.6/\text{mm}^2$) than in the contralateral striatum of the same animals ($336.5 \pm 20.5/\text{mm}^2$; $p < 0.05$) or in the ipsilateral striatum of sham-operated rats ($p < 0.05$). Minocycline treatment significantly increased the number of intact microvessels in the ipsilateral striatum (to $325.7 \pm 31.7/\text{mm}^2$; $p < 0.05$) compared with vehicle-treated ICH rats. The number of intact vessels in the contralateral striatum of minocycline-treated rats was $345.7 \pm 34.2/\text{mm}^2$. As an additional indicator of BBB disruption, extravasation of the blood protein, IgG, was monitored in the ipsilateral striatum 3 days after ICH onset (Fig. 1E). In vehicle-treated animals, IgG staining was widespread around the hematoma, with many small IgG-positive cells (probably microglia) at the edge. Minocycline treatment reduced both the diffuse and cellular IgG staining.

Effects of ICH and minocycline on cytokine and MMP expression

Expression of several genes was monitored using quantitative real-time RT-PCR (Fig. 2). Two pro-inflammatory cytokines (TNF α , IL1 β) and matrix metalloproteinases (MMP-3, MMP-9) were selected because of their link to BBB damage in other models of brain injury (Fujimura et al., 1999; Gasche et al., 1999; Gurney et al., 2006), and MMP-12 was monitored because of its reported up-regulation after ICH (Power et al., 2003). CR3 mRNA expression was used as an indicator of microglial activation and macrophage infiltration. The time course was chosen to begin after the hematoma had reached its maximal size (6 h; Wasserman and Schlichter, 2007) and to extend to the time at which edema was monitored (3 days). First, ICH-induced changes in gene expression were compared between sham-operated and vehicle-treated ICH rats. CR3 mRNA expression was unchanged at 6 h, and then increased ~ 2 -fold by 1 day (n.s.) and ~ 6 -fold by 3 days ($p < 0.001$). IL1 β showed the greatest mRNA increase at 6 h (~ 30 -fold; $p < 0.001$) and then remained elevated ~ 10 -fold at 1 day ($p < 0.001$) and 3 days ($p < 0.001$). TNF α was rapidly up-regulated in a sustained manner; ~ 5 -fold at 6 h ($p < 0.05$) and 1 day ($p = 0.005$), and ~ 2.5 -fold at 3 days (n.s.). MMP-3 and MMP-9 did not change significantly at any of the times examined,

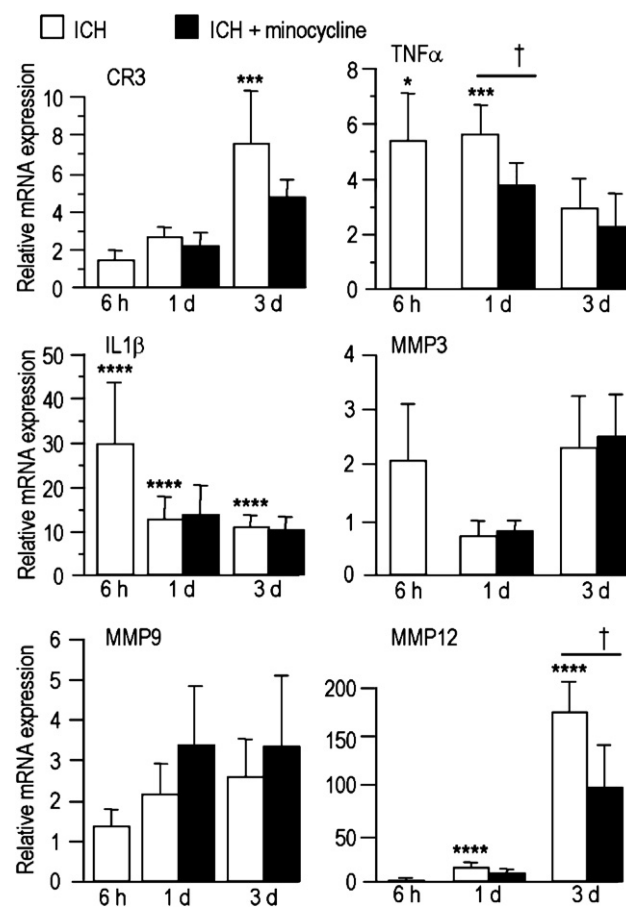


Fig. 2. Effects of ICH and minocycline on cytokine and MMP expression. Gene expression was measured by quantitative real-time RT-PCR in the ipsilateral (injured) striatum at 6 h, 1 day and 3 days after ICH onset. Transcript expression for each gene is shown as the fold increase relative to sham-operated (saline-injected) time-matched control rats. ICH-induced changes in gene expression are indicated as: * $p < 0.05$, ** $p < 0.01$, *** $p < 0.005$, **** $p < 0.001$; $n = 4-5$ for each treatment group. Note the huge increases in expression of matrix metalloproteinase-12 (MMP-12) and interleukin-1 β (IL1 β). Minocycline-treated animals received injections at 6 h (and at 1 and 2 days, if killed at 3 days). Minocycline reduced the expression of TNF α at 1 day and MMP-12 at 3 days, compared with vehicle-treated rats. † $p < 0.05$; $n = 4-5$ for each treatment group.

but MMP-9 showed an increasing trend (2 to 2.5-fold) at 1 and 3 days. In contrast, there was a massive increase in MMP-12 mRNA, which increased ~ 15 -fold by 1 day ($p < 0.001$) and ~ 175 -fold by 3 days ($p = 0.001$). Next, vehicle-treated ICH animals were compared with those receiving minocycline beginning at 6 h after ICH. Minocycline significantly decreased the ICH-induced TNF α up-regulation at 1 day; from a 5.8 ± 0.8 -fold up-regulation to 3.6 ± 1 -fold ($p < 0.05$, $n = 5$). Minocycline decreased the MMP-12 mRNA at 3 days; from a 175 ± 31 -fold up-regulation to 97 ± 44 -fold ($p < 0.05$, $n = 5$).

Cellular localization of TNF α and MMP-12

TNF α can be produced by a variety of brain cells (neurons, astrocytes, microglia, endothelial cells) and by infiltrating peripheral leukocytes, including neutrophils (Botchkina et al., 1997; Dziewulska and Mossakowski, 2003; Mayne et al., 2001b; Sairanen et al., 2001a,b). We assessed the cellular

location of TNF α protein by immunohistochemistry at 6 h, and 1 and 3 days after ICH onset (Fig. 3). In the contralateral striatum, no TNF α protein was detected at any of these times (Fig. 3A). In the ipsilateral striatum, very little TNF α protein was seen at 6 h, but by 1 day it was abundant at the edge of the hematoma, and also present in the adjacent intact striatum. By 3 days, TNF α immunoreactivity had increased at the edge of the hematoma, but was lower in the adjacent striatum. Labeling with TNF α and a marker for neutrophils (MPO) showed that most of the TNF α -positive cells were neutrophils at all times examined. Neutrophils (small, round, MPO-positive cells) were predominantly

found in a band at the edge of the hematoma, although some were scattered throughout the surrounding striatum, particularly at 1 day. A small number of TNF α -positive neutrophils were first seen in blood vessels surrounding the hematoma at 6 h (not shown). By 1 day (Fig. 3B), many TNF α -positive neutrophils (note their small size) were observed inside the parenchyma, and by 3 days (Fig. 3D) they were abundant at the edge of the hematoma. In minocycline-treated animals, the number of TNF α -positive neutrophils decreased at 1 day (Fig. 3C) and 3 days (Fig. 3E). Microglia/macrophages are much larger than neutrophils, and essentially all of them appear to be activated by 3 days, as judged by their enlarged cell bodies and short, retracted processes (Fig. 3F). Such morphological evidence of microglia activation was seen as early as 6 h (not shown). While TNF α was abundant on day 3, little if any co-localized with the microglia/macrophage marker (Iba1); instead, the staining was consistent with small round neutrophils scattered among the microglia/macrophages. The densities of TNF α -positive cells and neutrophils were quantified at the periphery of the hematoma at 1 and 3 days, with and without minocycline treatment (Fig. 3G). Minocycline significantly reduced the number of TNF α -positive cells (compared with vehicle-treated animals) at both 1 day (341 ± 78 vs. 205 ± 38 per mm^2 , $p < 0.05$) and 3 days (488 ± 61 vs. 255 ± 53 per mm^2 , $p < 0.005$). The degree of reduction by minocycline in numbers of TNF α -positive cells closely correlated with the reduced numbers of neutrophils; i.e., 517 ± 59 vs. 330 ± 47 per mm^2 ($p < 0.005$) at 1 day, and 949 ± 130 vs. 585 ± 122 per mm^2 ($p < 0.05$) at 3 days.

Matrix metalloprotease-12 can degrade collagen type IV in the basal lamina of cerebral blood vessels (Yong et al., 2001). Because minocycline reduced expression of MMP-12 mRNA and the loss of microvessels, it was important to determine the cellular source of MMP-12 protein. In the undamaged contralateral hemisphere, no MMP-12 staining was detected in either the striatum (Figs. 4A, D, F) or cortex (not shown). In contrast, there was considerable MMP-12 immunoreactivity throughout the ipsilateral striatum surrounding the hematoma at 1 and 3 days after ICH (Figs. 4B, C, E, G). MMP-12 staining co-localized with

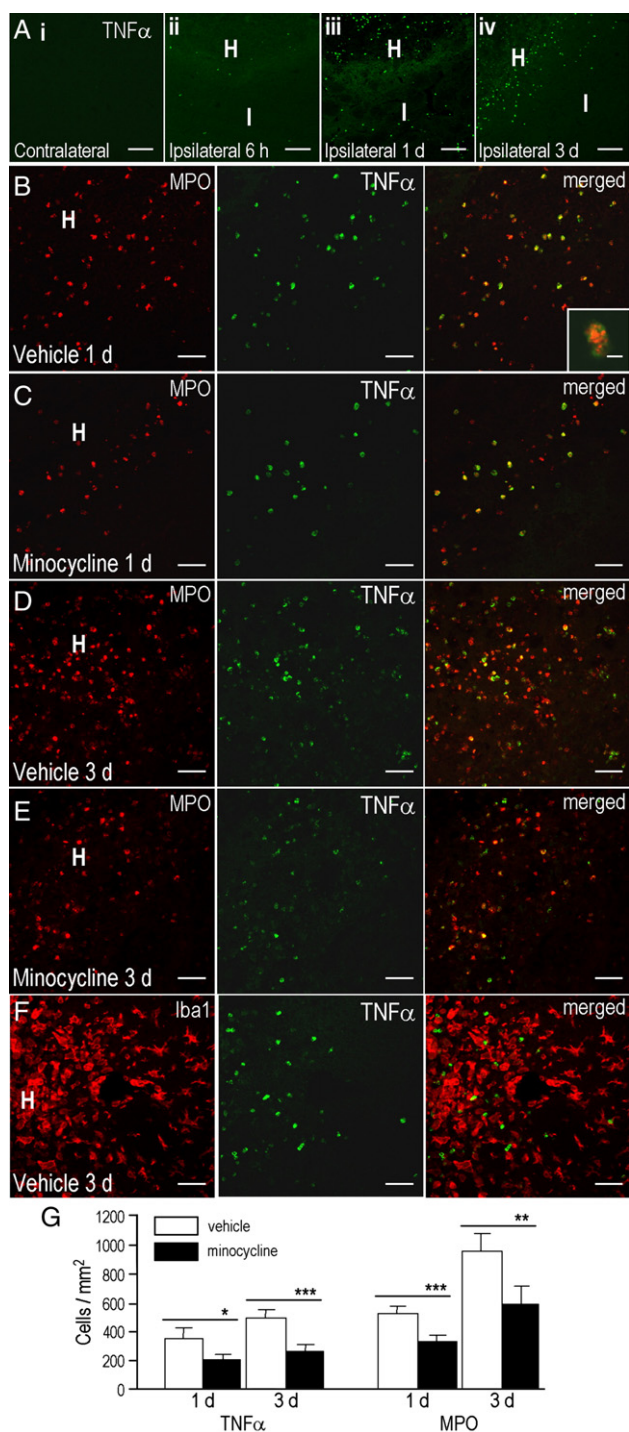


Fig. 3. Neutrophils are the major TNF α expressing cells. Brain sections were double labeled with an antibody against TNF α and markers for neutrophils (myeloperoxidase, MPO) or microglia/macrophages (ionized calcium binding adapter-1, Iba1). (A) Spatial and temporal profile of TNF α production. NB: No TNF α protein was detected in the contralateral hemisphere (panel i) at any time examined. In the ipsilateral striatum, a small number of TNF α -positive cells were first observed inside the hematoma (H) and in the adjacent 'intact' striatum (I) at 6 h (panel ii). By 1 day, more TNF α -positive cells were located inside the hematoma and the surrounding striatum (panel iii) whereas by 3 days, TNF α -positive cells were mainly located in a band at the periphery of the hematoma (panel iv). Scale bars, 150 μm . (B–E) Co-localization of TNF α with the neutrophil marker, MPO, at 1 day (B, C) and 3 days (D, E) after ICH. The inset in B is a higher magnification image of a neutrophil, showing punctate MPO and diffuse TNF α staining. After minocycline treatment, fewer TNF α -positive neutrophils were observed at 1 day (C) and 3 days (E) after ICH at the periphery of the hematoma. Scale bars: 50 μm ; inset, 10 μm . (F) Double labeling for TNF α and macrophages/microglia at the edge of the hematoma 3 days after ICH onset. Scale bars, 50 μm . (G) Quantitative analysis shows a significant reduction in numbers of MPO-positive and TNF α -positive cells at the periphery of the hematoma after minocycline treatment (* $p < 0.05$, ** $p < 0.01$, *** $p < 0.005$). $n = 4$ for each treatment group.

collagen type IV on blood vessels adjacent to the hematoma, increased with time and was clearly associated with vessel fragmentation. At the edge of the hematoma, MMP-12 was detected in Iba1-positive activated microglia/macrophages at 1 day (Fig. 4E). At 3 days after ICH, despite the large number of activated microglia/macrophages surrounding the hematoma

(Wasserman and Schlichter, 2007), they expressed little MMP-12 (not shown), whereas MAP-2-positive neurons robustly expressed MMP-12 (Fig. 4G). An intriguing observation was that MMP-12 expressing neurons generally had reduced MAP-2 staining (see inset) but were not dead or dying, since they did not stain with Fluoro-jade (not shown). Of note, in infarcted tissue following ischemic stroke, a reduction or loss in MAP-2 staining has been reported.

Discussion

This work presents several novel findings. The results show for the first time that minocycline treatment, delayed to a clinically relevant starting time, protects the blood–brain barrier (BBB) after ICH. This protection was manifested by amelioration of three key processes; i.e., decreases in the number of disrupted microvessels, serum protein extravasation into the brain and cerebral edema. This is apparently the first report using collagen type IV expression in order to show reduced numbers of intact blood vessels outside the hematoma. We show additional new aspects of minocycline treatment. Minocycline reduced expression of two genes related to BBB damage and edema: $\text{TNF}\alpha$ at day 1, and MMP-12 at day 3. Importantly, the $\text{TNF}\alpha$ was mainly restricted to neutrophils, while MMP-12 protein was expressed in damaged microvessels surrounding the hematoma. The temporal and cellular expression of $\text{TNF}\alpha$ and MMP-12 support a model whereby $\text{TNF}\alpha$ from neutrophils leads to an increase in MMP-12 in microvessels, which causes vessel breakdown and edema.

Vasogenic edema is an increase in brain water content caused by abnormal movement of water, ions and plasma proteins into the brain (Klatzo, 1987). It occurs in two phases; the first involves water and ion transport through endothelial cells and, possibly, astrocytes and can occur even when the BBB remains physically intact. This process might explain why, in the present study, the brain water content increased on the contralateral side without extravasation of IgG or disruption of the basal lamina. In the second phase, the BBB becomes physically disrupted, after which plasma proteins and water directly enter the brain, driven by hydrostatic and osmotic pressures (Simard et al., 2007). The physical integrity of the BBB is supported by the basal lamina, which is comprised primarily of collagen type IV, laminin and fibronectin. Although ischemic stroke and traumatic brain injury

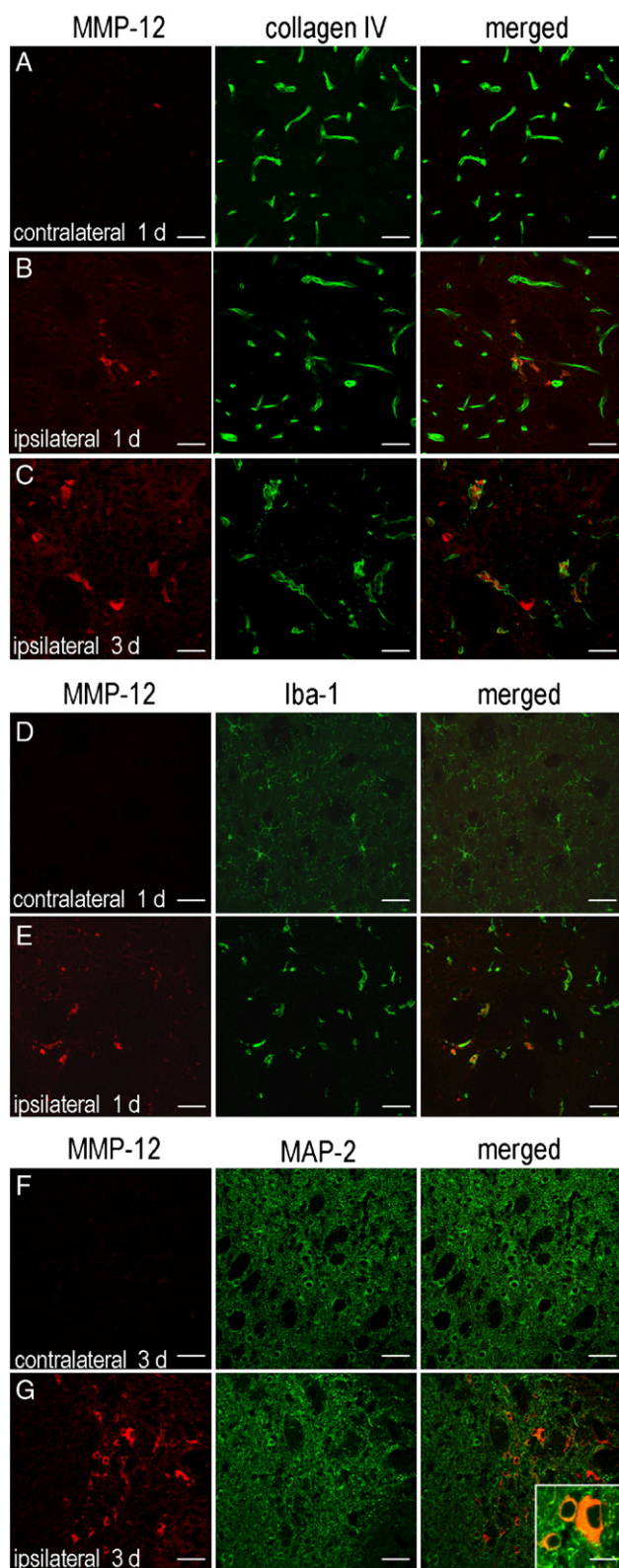


Fig. 4. Co-localization of MMP-12 protein with microvessels and neurons. On the days indicated in each panel, frozen brain sections were labeled with an antibody against MMP-12, and a second marker: collagen type IV for microvessels, Iba1 for microglia/macrophages or MAP-2 for neurons. Scale bars, 50 μm . (A) Microvessels had normal morphology in the uninjured contralateral striatum (collagen type IV staining) and lacked MMP-12. (B, C) On the ipsilateral side, many microvessels at the periphery of the hematoma were fragmented and most of these expressed MMP-12. (D) In the contralateral striatum, Iba1-positive cells (microglia) were highly ramified and did not express MMP-12. (E) In the ipsilateral striatum at the periphery of the hematoma, Iba1-positive cells had short processes and large cell bodies, and some expressed MMP-12. (F) In the contralateral striatum, MAP-2-positive neurons did not express MMP-12. (G) In the ipsilateral striatum, at the periphery of the hematoma, MMP-12 co-localized with MAP-2-positive neurons (inset shows magnified image (scale bar, 15 μm)).

are associated with loss of collagen type IV (Hamann et al., 2002, 2004; Muellner et al., 2003), little was known about the role of the basal lamina after ICH. We now provide evidence that ICH causes loss of microvessel integrity in the parenchyma surrounding the hematoma, suggesting that degradation of collagen type IV contributes to the observed opening of the BBB in the parenchyma surrounding the hematoma in humans (Lampf et al., 2005). Because this degradation was temporally and spatially associated with IgG extravasation and increased brain water content (edema), breakdown of the basal lamina is implicated in development of the vasogenic edema.

After ICH, abnormal fluid accumulation in the parenchyma caused by vasogenic edema appears to be an important mediator of secondary injury and clinical deterioration (Leira et al., 2004; Xi et al., 2006). In humans, edema is associated with increased intracranial pressure, cerebral hypertension and herniation. In both rats and humans, edema begins within hours and peaks in 3–4 days after ICH onset, although because of the larger amount of white matter, edema can peak as late as 10–20 days in the human brain. Because the BBB remains impermeable to large molecules for as much as 8–12 h after ICH onset (Xi et al., 2006), edema may be amenable to treatment. Although commonly used to treat cerebral edema, hyper-osmotic therapy (mannitol or hypertonic saline) is associated with serious side effects such as a rebound elevation in intracranial pressure, and it does not prevent further BBB damage (Knapp, 2005). Most importantly, our results suggest that minocycline protects the BBB by preventing disruption of the basal lamina and reducing movement of plasma proteins and water into the brain, even when treatment was delayed by 6 h after ICH onset. These results on minocycline have broader implications since edema is associated with degradation of the basal lamina in other models of brain injury, including ischemic stroke and trauma (Hamann et al., 2002, 2004; Muellner et al., 2003). Although previous studies of ICH did not demonstrate significant increases in neuron survival when rats were treated with minocycline (Power et al., 2003; Szymanska et al., 2006; Wasserman and Schlichter, 2007), the reduction we show in BBB damage and edema may have greater clinical relevance than neuron survival.

We found that IL1 β and TNF α mRNA were up-regulated within hours of ICH onset, a time course that is consistent with their putative role as ‘orchestrators’ of the inflammatory response. Both cytokines have been implicated in BBB damage, and they initiate events leading to neutrophil recruitment into the brain (de Vries et al., 1996; Didier et al., 2003; Megyeri et al., 1992; Wong et al., 2004; Wright and Merchant, 1994). Even in the absence of a stroke, injecting either cytokine causes neutrophil infiltration, BBB disruption and vasogenic edema (Holmin and Mathiesen, 2000). Moreover, high plasma levels of TNF α within 24 h of hematoma onset are associated with increased perihematoma edema in humans (Castillo et al., 2002). Although minocycline reduced expression of IL1 β and TNF α after ischemic stroke (Lai and Todd, 2006; Ledebuer et al., 2005), it may not be as effective after ICH; it reduced TNF α but not IL1 β in the present study. It remains possible that minocycline can alter IL1 β activity since it reduces expression of interleukin-1 converting enzyme (Yrjanheikki et al., 1998). The reported

cellular sources of TNF α include microglia/macrophages, neutrophils, astrocytes, endothelial cells or neurons in different models of brain injury. TNF α protein was detected in neutrophils and microglia/macrophages after ICH (Mayne et al., 2001b), whereas we observed it mainly in neutrophils and very rarely in microglia/macrophages from 1 to 3 days after ICH. After permanent ischemia, TNF α mRNA was observed mainly in activated microglia/macrophages, with none in neutrophils (Gregersen et al., 2000). Such differences might reflect temporal changes or detection difficulties. Because neutrophils contain pre-made TNF α in intracellular stores, detecting its immunoreactivity should be relatively easy. However, if other cell types simultaneously produce and secrete TNF α , the cellular concentration might simply be below the detection level of the antibody.

Targeting neutrophils to protect the BBB seems a reasonable strategy, based on their large numbers, high TNF α production and the effect of minocycline on neutrophil infiltration and BBB disruption. Minocycline inhibits neutrophil chemotaxis (Sugita and Nishimura, 1995), and decreasing the neutrophil burden is a unifying mechanism with other therapeutic strategies that reduce edema following experimental ICH, including hypothermia (MacLellan et al., 2006), depleting systemic complement (Xi et al., 2001) and inhibiting IL1 β signaling (Masada et al., 2001). Importantly, delayed treatments can reduce neutrophil infiltration and BBB disruption: 6 h for minocycline (present study) and 1–4 h for hypothermia (MacLellan et al., 2006). Since TNF α is a potent neutrophil activator, and reduced by minocycline, this treatment is expected to reduce other neutrophil products that can damage the BBB, including oxygen metabolites and proteases (Scholz et al., 2007).

Matrix metalloproteinases (MMPs) have been widely implicated as mediators of BBB damage; e.g., in ischemic and hemorrhagic stroke, traumatic brain and spinal cord injury, and multiple sclerosis (Yong et al., 2001). After experimental ICH, broad spectrum MMP inhibitors reduced brain injury, BBB disruption and edema (Rosenberg and Navratil, 1997; Wang and Tsirka, 2005), but ischemic and hemorrhagic stroke may differ in the cellular expression profile of specific MMP types. After ischemic stroke, the levels and activities of MMP-2 and MMP-9 correlated with loss of microvessel integrity, which was abrogated by treatments that decreased MMPs; i.e., broad-spectrum MMP inhibitors, hypothermia or minocycline (Hamann et al., 2004; Machado et al., 2006; Sumii and Lo, 2002). Following ICH in humans, an increase in plasma MMP-9 correlates with perihematoma edema and early neurological deterioration (Abilleira et al., 2003). However, MMP-2 and MMP-9 may not be appropriate therapeutic targets because they are normally expressed by various brain cell types and likely play a role in normal brain physiology.

MMP-12 is not expressed in the healthy brain; thus, inhibiting it should have fewer side effects than a broad-spectrum MMP inhibitor (Zhao et al., 2006). MMP-12 expression has not been assessed after ICH in humans, but in animal models, it appears to be a strong marker of brain injury. Two earlier studies show that it is the most highly up-regulated MMP of those examined after ICH, that MMP-12 reduction by minocycline correlates with improved functional recovery (Power et al., 2003), and that

MMP-12 deficient mice have better sensorimotor recovery (Wells et al., 2005). The time course of MMP-12 expression differs in these studies. Wells et al. (2005) showed increased expression at 1 day and a peak at 5 days (other days were not examined), whereas Power et al. (2003) observed MMP-12 up-regulation only at 7 days and saw a reduction by minocycline. We found that MMP-12 increased significantly at 1 day, and that the much larger increase at 3 days was reduced by minocycline. The discrepancy in timing between the present study and Power et al. (2003) very likely reflect the different locations of tissue sampled for real-time RT-PCR. Because inflammation occurs immediately adjacent to the hematoma, we sampled the hematoma and surrounding striatum. Power et al. (2003) sampled a more remote location, 2–4 mm from the edge of the hematoma, and thus underestimated early inflammatory events. Nevertheless, from these studies using the same model of ICH, it appears that MMP-12 is the most highly up-regulated MMP, and that its expression rises first close to the hematoma (day 1), and then later in more distal tissue (day 7). A similar spatial difference is likely to exist for IL1 β expression, because we observed a ~30-fold mRNA increase in proximal tissue (this study) compared with the previously reported <2-fold increase in distal tissue (Power et al., 2003). Finally, our observation that minocycline reduced TNF α at 1 day (before it reduced MMP-12), may explain why Power et al. (2003) observed some neurological improvement in minocycline-treated rats at day 1, even though the differences were not statistically significant until day 7.

MMP-12 can be produced by a variety of brain cells (Hummel et al., 2001; Power et al., 2003; Vos et al., 2003; Wells et al., 2003) and might be a critical target for reducing BBB damage after ICH since it can degrade collagen type IV (Yong et al., 2001). However, it was not known whether the cellular source changes with time after ICH. We detected MMP-12 in microvessels surrounding the hematoma at 1 and 3 days, and we found that MMP-12 containing microvessels became fragmented at the time when edema in this region reached a peak. Thus, we show for the first time that MMP-12 is in the right place at the right time to degrade the basal lamina, and contribute to the development of edema after ICH. In addition, we detected MMP-12 in microglia/macrophages at day 1 and show for the first time that it is robustly expressed in neurons. A previous study (Power et al., 2003) showed MMP-12 in microglia/macrophages at a later time (7 days). It remains to be elucidated whether these different cellular sources of MMP-12 contribute differently to brain injury.

Our results suggest a sequential mechanism after ICH, whereby TNF α leads to an increase in MMP-12, which further degrades the basal lamina surrounding the hematoma and disrupts the BBB. That is, we observed TNF α protein in neutrophils and MMP-12 protein in damaged microvessels surrounding the hematoma and found that minocycline first decreased TNF α expression and then decreased MMP-12 expression. This is consistent with promotion of MMP transcription by inflammatory cytokines, including TNF α (Borden and Heller, 1997), but does not preclude involvement of other cell types and molecules. Minocycline likely protects the BBB by inhibiting the cumulative effect of TNF α production by a variety of cell types (Mayne et al., 2001b)

and preventing loss of collagen type IV, but it also reduces activation of microglia, production of reactive oxygen species (Yenari et al., 2006), and decreases the number of infiltrating neutrophils (Wasserman and Schlichter, 2007). We found that minocycline did not fully restore the normal brain water content after ICH; thus, targeting several mechanisms, including direct inhibition of neutrophils and MMP-12, may prove more clinically effective.

Acknowledgments

Excellent technical help was provided by X-P Zhu and H Yang. We are grateful for comments from Drs. J Eubanks, L Mills and EF Stanley. Supported by grants to LCS from the Heart and Stroke Foundation (HSFO; NA5158, T5546), Krembil Scientific Development Seed Fund, Canadian Stroke Network and a scholarship to JW from HSF Canada.

References

- Abilleira, S., Montaner, J., Molina, C.A., Monasterio, J., Castillo, J., Alvarez-Sabin, J., 2003. Matrix metalloproteinase-9 concentration after spontaneous intracerebral hemorrhage. *J. Neurosurg.* 99, 65–70.
- Borden, P., Heller, R.A., 1997. Transcriptional control of matrix metalloproteinases and the tissue inhibitors of matrix metalloproteinases. *Crit. Rev. Eukaryot. Gene Expr.* 7, 159–178.
- Barone, F.C., Feuerstein, G.Z., 1999. Inflammatory mediators and stroke: new opportunities for novel therapeutics. *J. Cereb. Blood Flow Metab.* 19, 819–834.
- Botchkina, G.I., Meistrell III, M.E., Botchkina, I.L., Tracey, K.J., 1997. Expression of TNF and TNF receptors (p55 and p75) in the rat brain after focal cerebral ischemia. *Mol. Med.* 3, 765–781.
- Bustin, S.A., Nolan, T., 2004. Pitfalls of quantitative real-time reverse-transcription polymerase chain reaction. *J. Biomol. Tech.* 15, 155–166.
- Castillo, J., Davalos, A., varez-Sabin, J., Pumar, J.M., Leira, R., Silva, Y., Montaner, J., Kase, C.S., 2002. Molecular signatures of brain injury after intracerebral hemorrhage. *Neurology* 58, 624–629.
- de Vries, H.E., Blom-Roosmalen, M.C., van, O.M., de Boer, A.G., van Berkel, T.J., Breimer, D.D., Kuiper, J., 1996. The influence of cytokines on the integrity of the blood–brain barrier in vitro. *J. Neuroimmunol.* 64, 37–43.
- Didier, N., Romero, I.A., Creminon, C., Wijkhuizen, A., Grassi, J., Mabondzo, A., 2003. Secretion of interleukin-1beta by astrocytes mediates endothelin-1 and tumour necrosis factor-alpha effects on human brain microvascular endothelial cell permeability. *J. Neurochem.* 86, 246–254.
- Dziewulska, D., Mossakowski, M.J., 2003. Cellular expression of tumor necrosis factor α and its receptors in human ischemic stroke. *Clin. Neuropathol.* 22, 35–40.
- Elewa, H.F., Hilali, H., Hess, D.C., Machado, L.S., Fagan, S.C., 2006. Minocycline for short-term neuroprotection. *Pharmacotherapy* 26, 515–521.
- Feuerstein, G.Z., Wang, X., Barone, F.C., 1998. The role of cytokines in the neuropathology of stroke and neurotrauma. *Neuroimmunomodulation* 5, 143–159.
- Fujimura, M., Gasche, Y., Morita-Fujimura, Y., Massengale, J., Kawase, M., Chan, P.H., 1999. Early appearance of activated matrix metalloproteinase-9 and blood–brain barrier disruption in mice after focal cerebral ischemia and reperfusion. *Brain Res.* 842, 92–100.
- Gasche, Y., Fujimura, M., Morita-Fujimura, Y., Copin, J.C., Kawase, M., Massengale, J., Chan, P.H., 1999. Early appearance of activated matrix metalloproteinase-9 after focal cerebral ischemia in mice: a possible role in blood–brain barrier dysfunction. *J. Cereb. Blood Flow Metab.* 19, 1020–1028.
- Gregersen, R., Lambertsen, K., Finsen, B., 2000. Microglia and macrophages are the major source of tumor necrosis factor in permanent middle cerebral artery occlusion in mice. *J. Cereb. Blood Flow Metab.* 20, 53–65.
- Gurney, K.J., Estrada, E.Y., Rosenberg, G.A., 2006. Blood–brain barrier

- disruption by stromelysin-1 facilitates neutrophil infiltration in neuroinflammation. *Neurobiol. Dis.* 23, 87–96.
- Hamann, G.F., Liebetrau, M., Martens, H., Burggraf, D., Kloss, C.U., Bultemeier, G., Wunderlich, N., Jager, G., Pfefferkorn, T., 2002. Microvascular basal lamina injury after experimental focal cerebral ischemia and reperfusion in the rat. *J. Cereb. Blood Flow Metab.* 22, 526–533.
- Hamann, G.F., Burggraf, D., Martens, H.K., Liebetrau, M., Jager, G., Wunderlich, N., DeGeorgia, M., Krieger, D.W., 2004. Mild to moderate hypothermia prevents microvascular basal lamina antigen loss in experimental focal cerebral ischemia. *Stroke* 35, 764–769.
- Hewlett, K.A., Corbett, D., 2006. Delayed minocycline treatment reduces long-term functional deficits and histological injury in a rodent model of focal ischemia. *Neuroscience* 141, 27–33.
- Holmin, S., Mathiesen, T., 2000. Intracerebral administration of interleukin-1beta and induction of inflammation, apoptosis, and vasogenic edema. *J. Neurosurg.* 92, 108–120.
- Hua, Y., Wu, J., Keep, R.F., Nakamura, T., Hoff, J.T., Xi, G., 2006. Tumor necrosis factor-alpha increases in the brain after intracerebral hemorrhage and thrombin stimulation. *Neurosurgery* 58, 542–550.
- Hummel, V., Kallmann, B.A., Wagner, S., Fuller, T., Bayas, A., Tonn, J.C., Benveniste, E.N., Toyka, K.V., Rieckmann, P., 2001. Production of MMPs in human cerebral endothelial cells and their role in shedding adhesion molecules. *J. Neuropathol. Exp. Neurol.* 60, 320–327.
- Kaushal, V., Koeberle, P.D., Wang, Y., Schlichter, L.C., 2007. The Ca²⁺-activated K⁺ channel KCNN4/KCa3.1 contributes to microglia activation and nitric oxide-dependent neurodegeneration. *J. Neurosci.* 27, 234–244.
- Klatzo, I., 1987. Pathophysiological aspects of brain edema. *Acta Neuropathol. (Berl)* 72, 236–239.
- Knapp, J.M., 2005. Hyperosmolar therapy in the treatment of severe head injury in children: mannitol and hypertonic saline. *AACN Clin. Issues* 16, 199–211.
- Lai, A.Y., Todd, K.G., 2006. Hypoxia-activated microglial mediators of neuronal survival are differentially regulated by tetracyclines. *Glia* 53, 809–816.
- Lampl, Y., Shmuilovich, O., Lockman, J., Sadeh, M., Lorberboym, M., 2005. Prognostic significance of blood brain barrier permeability in acute hemorrhagic stroke. *Cerebrovasc. Dis.* 20, 433–437.
- Ledeboer, A., Sloane, E.M., Milligan, E.D., Frank, M.G., Mahony, J.H., Maier, S.F., Watkins, L.R., 2005. Minocycline attenuates mechanical allodynia and proinflammatory cytokine expression in rat models of pain facilitation. *Pain* 115, 71–83.
- Leira, R., Davalos, A., Silva, Y., Gil-Peralta, A., Tejada, J., Garcia, M., Castillo, J., 2004. Early neurologic deterioration in intracerebral hemorrhage: predictors and associated factors. *Neurology* 63, 461–467.
- Machado, L.S., Kozak, A., Ergul, A., Hess, D.C., Borlongan, C.V., Fagan, S.C., 2006. Delayed minocycline inhibits ischemia-activated matrix metalloproteinases 2 and 9 after experimental stroke. *BMC Neurosci.* 17, 56.
- MacLellan, C.L., Girgis, J., Colbourne, F., 2004. Delayed onset of prolonged hypothermia improves outcome after intracerebral hemorrhage in rats. *J. Cereb. Blood Flow Metab.* 24, 432–440.
- MacLellan, C.L., Davies, L.M., Fingas, M.S., Colbourne, F., 2006. The influence of hypothermia on outcome after intracerebral hemorrhage in rats. *Stroke* 37, 1266–1270.
- Maier, C.M., Hsieh, L., Crandall, T., Narasimhan, P., Chan, P.H., 2006. Evaluating therapeutic targets for reperfusion-related brain hemorrhage. *Ann. Neurol.* 59, 929–938.
- Masada, T., Hua, Y., Xi, G., Yang, G.Y., Hoff, J.T., Keep, R.F., 2001. Attenuation of intracerebral hemorrhage and thrombin-induced brain edema by overexpression of interleukin-1 receptor antagonist. *J. Neurosurg.* 95, 680–686.
- Mayer, S.A., Rincon, F., 2005. Treatment of intracerebral haemorrhage. *Lancet Neurol.* 4, 662–672.
- Mayne, M., Fotheringham, J., Yan, H.J., Power, C., Del Bigio, M.R., Peeling, J., Geiger, J.D., 2001a. Adenosine A2A receptor activation reduces proinflammatory events and decreases cell death following intracerebral hemorrhage. *Ann. Neurol.* 49, 727–735.
- Mayne, M., Ni, W., Yan, H.J., Xue, M., Johnston, J.B., Del Bigio, M.R., Peeling, J., Power, C., 2001b. Antisense oligodeoxynucleotide inhibition of tumor necrosis factor-alpha expression is neuroprotective after intracerebral hemorrhage. *Stroke* 32, 240–248.
- Megyeryi, P., Abraham, C.S., Temesvari, P., Kovacs, J., Vas, T., Speer, C.P., 1992. Recombinant human tumor necrosis factor alpha constricts pial arterioles and increases blood–brain barrier permeability in newborn piglets. *Neurosci. Lett.* 148, 137–140.
- Middleton, J., Patterson, A.M., Gardner, L., Schmutz, C., Ashton, B.A., 2002. Leukocyte extravasation: chemokine transport and presentation by the endothelium. *Blood* 100, 3853–3860.
- Muellner, A., Benz, M., Kloss, C.U., Mautes, A., Burggraf, D., Hamann, G.F., 2003. Microvascular basal lamina antigen loss after traumatic brain injury in the rat. *J. Neurotrauma* 20, 745–754.
- Power, C., Henry, S., Del Bigio, M.R., Larsen, P.H., Corbett, D., Imai, Y., Yong, V.W., Peeling, J., 2003. Intracerebral hemorrhage induces macrophage activation and matrix metalloproteinases. *Ann. Neurol.* 53, 731–742.
- Qureshi, A.I., Tuhrim, S., Broderick, J.P., Batjer, H.H., Hondo, H., Hanley, D.F., 2001. Spontaneous intracerebral hemorrhage. *N. Engl. J. Med.* 344, 1450–1460.
- Rincon, F., Mayer, S.A., 2004. Novel therapies for intracerebral hemorrhage. *Curr. Opin. Crit. Care* 10, 94–100.
- Rosenberg, G.A., 2002. Matrix metalloproteinases in neuroinflammation. *Glia* 39, 279–291.
- Rosenberg, G.A., Navratil, M., 1997. Metalloproteinase inhibition blocks edema in intracerebral hemorrhage in the rat. *Neurology* 48, 921–926.
- Rosenberg, G.A., Mun-Bryce, S., Wesley, M., Kornfeld, M., 1990. Collagenase-induced intracerebral hemorrhage in rats. *Stroke* 21, 801–807.
- Sairanen, T., Carpen, O., Karjalainen-Lindsberg, M.L., Paetau, A., Turpeinen, U., Kaste, M., Lindsberg, P.J., 2001a. Evolution of cerebral tumor necrosis factor-alpha production during human ischemic stroke. *Stroke* 32, 1750–1758.
- Sairanen, T.R., Lindsberg, P.J., Brenner, M., Carpen, O., Siren, A., 2001b. Differential cellular expression of tumor necrosis factor-alpha and Type I tumor necrosis factor receptor after transient global forebrain ischemia. *J. Neurol. Sci.* 186, 87–99.
- Sanchez Mejia, R.O., Ona, V.O., Li, M., Friedlander, R.M., 2001. Minocycline reduces traumatic brain injury-mediated caspase-1 activation, tissue damage, and neurological dysfunction. *Neurosurgery* 48, 1393–1399.
- Scholz, M., Cinatl, J., Schadel-Hopfner, M., Windolf, J., 2007. Neutrophils and the blood–brain barrier dysfunction after trauma. *Med. Res. Rev.* 27, 401–416.
- Simard, J.M., Kent, T.A., Chen, M., Tarasov, K.V., Gerzanich, V., 2007. Brain oedema in focal ischaemia: molecular pathophysiology and theoretical implications. *Lancet Neurol.* 6, 258–268.
- Stirling, D.P., Koochesfahani, K.M., Steeves, J.D., Tetzlaff, W., 2005. Minocycline as a neuroprotective agent. *Neuroscientist* 11, 308–322.
- Sugita, K., Nishimura, T., 1995. Effect of antimicrobial agents on chemotaxis of polymorphonuclear leukocytes. *J. Chemother.* 7, 118–125.
- Sumii, T., Lo, E.H., 2002. Involvement of matrix metalloproteinase in thrombolysis-associated hemorrhagic transformation after embolic focal ischemia in rats. *Stroke* 33, 831–836.
- Szymanska, A., Biernaskie, J., Laidley, D., Granter-Button, S., Corbett, D., 2006. Minocycline and intracerebral hemorrhage: influence of injury severity and delay to treatment. *Exp. Neurol.* 197, 189–196.
- Tanno, H., Nockels, R.P., Pitts, L.H., Noble, L.J., 1992. Breakdown of the blood–brain barrier after fluid percussive brain injury in the rat. Part 1: Distribution and time course of protein extravasation. *J. Neurotrauma* 9, 21–32.
- Vos, C.M., van Haastert, E.S., de Groot, C.J., van d. V., de Vries, H.E., 2003. Matrix metalloproteinase-12 is expressed in phagocytotic macrophages in active multiple sclerosis lesions. *J. Neuroimmunol.* 138, 106–114.
- Wang, J., Tsirka, S.E., 2005. Neuroprotection by inhibition of matrix metalloproteinases in a mouse model of intracerebral haemorrhage. *Brain* 128, 1622–1633.
- Wang, J., Dore, S., 2006. Inflammation after intracerebral hemorrhage. *J. Cereb. Blood Flow Metab.* 27, 894–908.
- Wasserman, J.K., Schlichter, L.C., 2007. Neuron death and inflammation in a rat model of intracerebral hemorrhage: Effects of delayed minocycline treatment. *Brain Res.* 1136, 208–218.

- Wells, J.E., Hurlbert, R.J., Fehlings, M.G., Yong, V.W., 2003. Neuroprotection by minocycline facilitates significant recovery from spinal cord injury in mice. *Brain* 126, 1628–1637.
- Wells, J.E., Biernaskie, J., Szymanska, A., Larsen, P.H., Yong, V.W., Corbett, D., 2005. Matrix metalloproteinase (MMP)-12 expression has a negative impact on sensorimotor function following intracerebral haemorrhage in mice. *Eur. J. Neurosci.* 21, 187–196.
- Wong, D., Dorovini-Zis, K., Vincent, S.R., 2004. Cytokines, nitric oxide, and cGMP modulate the permeability of an in vitro model of the human blood–brain barrier. *Exp. Neurol.* 190, 446–455.
- Wright, J.L., Merchant, R.E., 1994. Blood–brain barrier changes following intracerebral injection of human recombinant tumor necrosis factor-alpha in the rat. *J. Neurooncol.* 20, 17–25.
- Xi, G., Hua, Y., Keep, R.F., Younger, J.G., Hoff, J.T., 2001. Systemic complement depletion diminishes perihematomal brain edema in rats. *Stroke* 32, 162–167.
- Xi, G., Keep, R.F., Hoff, J.T., 2006. Mechanisms of brain injury after intracerebral haemorrhage. *Lancet Neurol.* 5, 53–63.
- Yenari, M.A., Xu, L., Tang, X.N., Qiao, Y., Giffard, R.G., 2006. Microglia potentiate damage to blood–brain barrier constituents: improvement by minocycline in vivo and in vitro. *Stroke* 37, 1087–1093.
- Yong, V.W., Power, C., Forsyth, P., Edwards, D.R., 2001. Metalloproteinases in biology and pathology of the nervous system. *Nat. Rev., Neurosci.* 2, 502–511.
- Yong, V.W., Wells, J., Giuliani, F., Casha, S., Power, C., Metz, L.M., 2004. The promise of minocycline in neurology. *Lancet Neurol.* 3, 744–751.
- Yrjanheikki, J., Keinanen, R., Pellikka, M., Hokfelt, T., Koistinaho, J., 1998. Tetracyclines inhibit microglial activation and are neuroprotective in global brain ischemia. *Proc. Natl. Acad. Sci. U. S. A.* 95, 15769–15774.
- Yrjanheikki, J., Tikka, T., Keinanen, R., Goldsteins, G., Chan, P.H., Koistinaho, J., 1999. A tetracycline derivative, minocycline, reduces inflammation and protects against focal cerebral ischemia with a wide therapeutic window. *Proc. Natl. Acad. Sci. U. S. A.* 96, 13496–13500.
- Zhang, W., Smith, C., Howlett, C., Stanimirovic, D., 2000. Inflammatory activation of human brain endothelial cells by hypoxic astrocytes in vitro is mediated by IL-1beta. *J. Cereb. Blood Flow Metab.* 20, 967–978.
- Zhao, B.Q., Wang, S., Kim, H.Y., Storrie, H., Rosen, B.R., Mooney, D.J., Wang, X., Lo, E.H., 2006. Role of matrix metalloproteinases in delayed cortical responses after stroke. *Nat. Med.* 12, 441–445.